Eidgenössische Materialprüfungs- und Forschungsanstalt
Laboratoire fédéral d'essai des matériaux et de recherche
Laboratorio federale di prova dei materiali e di ricerca
Institut federal da controlla da material e da retschertgas
Swiss Federal Laboratories for Materials Testing and Research

EMPA
Überlandstrasse 129
CH-8600 Dübendorf
Tel. +41-1-823 55 11
Fax +41-1-821 62 44

Analysis of Dynamic Wheel Load Signals in the Frequency Domain

by

Walter Krebs

Reto Cantieni

Section Concrete Structures

EMPA, Swiss Federal Laboratories for Materials Testing and Research

Duebendorf, Switzerland

Report presented at

Engineering Foundation Conference Vehicle - Infrastructure Interaction IV,

June 2 - 7, 1996, Bahia Resort Hotel, San Diego, California

Summary

In the context of the OECD DIVINE project (Dynamic Interaction Between Vehicle and Infrastructure Experiment), dynamic load tests were performed on three medium-span bridges in Switzerland. The test vehicle was a five-axle tractor-semitrailer with a 450 kN gross weight provided by the NRC, Center for Surface Transportation Technology, Ottawa. All ten wheels were instrumented to measure the dynamic wheel loads. The suspension system of the vehicle could be changed between steel leaf and air suspension, the dominant body bounce frequency hence changing between f ≈ 3 Hz and f ≈ 1.5 Hz. The three bridges tested were pre stressed concrete structures with maximal span lengths L = 31 m, 41 m, 70 m and fundamental natural frequencies f = 4.4 Hz, 3.0 Hz and 1.6 Hz respectively. Dynamic load tests were performed on all three bridges with the two suspension systems fitted to the test vehicle. Vehicle speed was kept constant during one specific test and the speed ranged from 5 to 80 km/h.

The digitized wheel load signals were subsequently analyzed in the frequency domain for more than 200 test runs. As a first step, the power spectral densities (PSD) were determined for every wheel. Next, for every peak in the PSD's the corresponding vehicle vibrational shape was determined, using a software package to animate and visualize the vibrational modes of the vehicle.

As expected, the analysis revealed that frequency coupling and hence interaction of the system vehicle/bridge occurs for the cases, where the fundamental frequencies of the two subsystems are close to each other, resulting in a reduction in the frequency of the coupled system. This frequency shift was clearly identified, for the steel leaf vehicle on the 3 Hz bridge. A small effect was observed for both suspension systems, when the vehicle passed the 1.6 Hz bridge. For the vehicle with steel leaf suspension, this may be explained by resonances with higher vibrational modes of the bridge. No frequency coupling can be observed in the other cases.

1. Introduction

Highway bridges are exposed to various loadings, when crossed by heavy commercial vehicles. In addition to the static effects due to the weight of the vehicle, bridges also exhibit dynamic responses to the passage of heavy vehicles. It is well known from earlier investigations, that the dynamic bridge response can become large, when the fundamental frequency of the bridge corresponds to the body bounce frequency of the vehicle. Furthermore, the pavement unevenness is a parameter of primary importance. In the case of "frequency matching" and medium to rough pavement quality the dynamic increment reaches values of up to 70% [1], [2].

Conventional vehicles equipped with steel leaf suspensions show fundamental wheel load frequencies in the range 2.5...3 Hz. As a consequence, their dynamic effect on bridges becomes large, when the fundamental frequency of the bridge is in the same range. This is the case for bridges with span lengths of about L = 40 m. Modern vehicles are most often equipped with low-friction or air suspensions. Such vehicles show predominant wheel load frequencies f ≈ 1.5...1.8 Hz. This frequency corresponds to the fundamental frequency of larger bridges with a span length of L = 70...80 m. The question arises, what additional loadings occur when bridges are crossed by vehicles with these new suspension systems.

To answer this question, the exact motion and vibration of vehicle and bridge have to be known as well as their interaction. Investigating these problems is the aim of the OECD project DIVINE (Dynamic Interaction between Vehicle and Infrastructure Experiment), Research Element 6, Bridge Research.

2. The OECD DIVINE Project

In the context of the OECD DIVINE project, dynamic load tests were performed on three medium-span bridges in Switzerland. The test vehicle was a five-axle tractor-semitrailer with a 450 kN gross weight provided by the National Research Council of Canada (NRC), Ottawa. All of the ten wheels of the test vehicle were instrumented to measure the dynamic wheel loads. The suspension system of the vehicle could be changed between steel leaf and air suspension, the dominant body bounce frequency hence changing

between f ≈ 3 Hz and f ≈ 1.5 Hz. For the experiment two bridges with natural frequencies corresponding to the frequency of the test vehicle equipped with steel leaf suspension and air suspension respectively were selected. To allow comparison with a "neutral, non-frequency-matching" bridge for either of the suspensions, a third bridge with a natural frequency of f = 4.4 Hz was also included in the tests. This bridge also provided a link between the OECD DIVINE experiments performed in Switzerland on medium-span bridges and those performed in Australia on short-span bridges.

2.1 The Test Vehicle

The test vehicle was a five-axle tractor-semi-trailer owned by NRC. Its geometry is given in Figure 1. For the tests only two of the trailer tank's four compartments were filled with water so that the vehicle gross weight was 450 kN. The individual axle loads are also indicated in Figure 1. The tyre type with the corresponding dynamic circumference is given in table 1.

The NRC test vehicle offers two features that make it most probably unique world-wide:

- Its suspension system can be interchanged between steel leaf and air suspension. This does not apply to the steer axle which is always equipped with a steel leaf suspension.
- All wheels are instrumented so that the dynamic wheel loads can be continuously measured.

The wheel load measurement instrumentation consists basically of shear gauges and accelerometers, both mounted on the axle close to the wheel hub. The method used to derive wheel load from the corresponding signals is described in detail in [3].

In addition to the wheel load measurement instrumentation the vehicle is equipped with sophisticated devices enabling the driver to accurately control the vehicle speed and to exactly identify the vehicle location on the test track. Both devices, operating with contactless optical sensors are activated by white, reflective strips glued on the pavement at distances of 30 m. At the start and end of the test track, four of these stripes were glued at distances of 190 mm from each other to trigger the on-board data acquisition system.

Axle Nr.	Tire type	Rolling circumference
1	Uniroyal 14/80 R20	3.478 m
2 and 3	Michelin 12R 22.5	3.302 m
4 and 5	Michelin 11R 22.5	3.213 m

Table 1 Tire type and dimensions of the test vehicle

2.2 The Bridges

The bridges tested in Switzerland in April/May 1994 were Föss, Deibüel and Sort bridge. All three are prestressed concrete structures with a one- or two-cell box girder cross section. The geometry of the bridges is shown in Figure 2, more detailed information is given in [4].

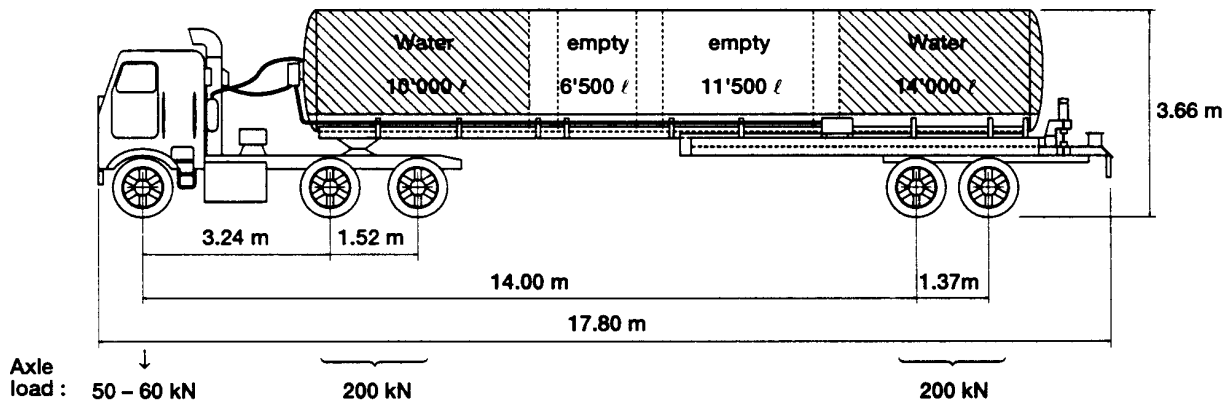

Fig. 1 The NRC Test Vehicle

Longitudinal views of the bridges tested

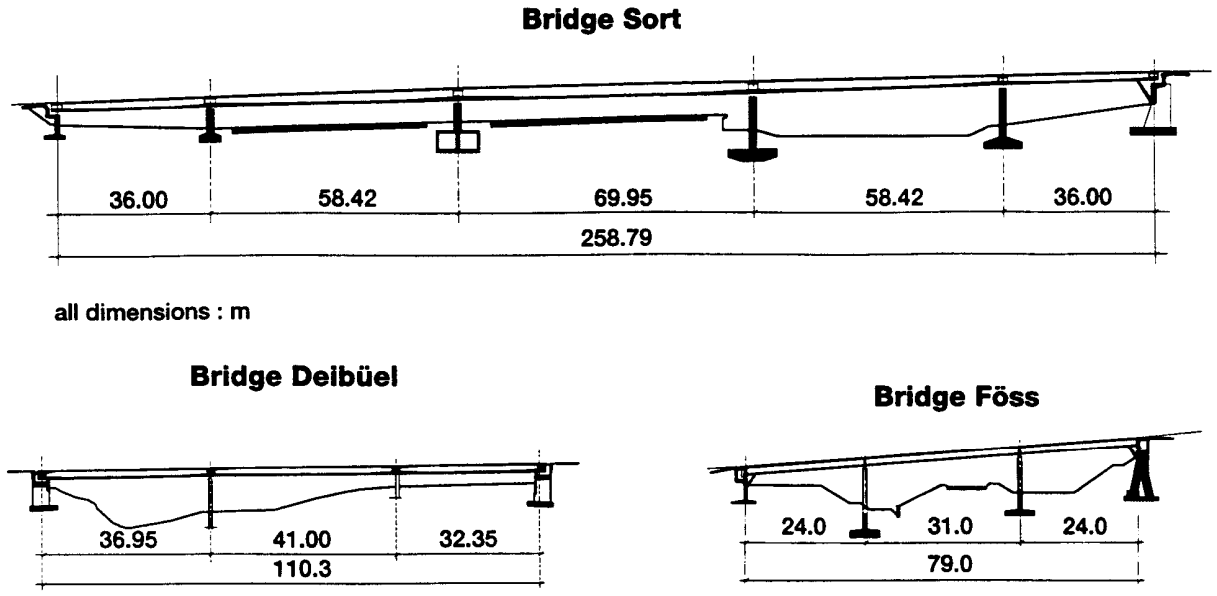

Fig. 2 Longitudinal section of the test bridges

Mode Nr.	Frequency [Hz] Föss		Deibüel		Sort	
1	4.03	H	3.01	B	1.04	H
2	4.44	B	3.79	V	1.62	B
3	6.45	B	4.24	B	1.73	H
4	7.10	T	5.43	B	2.45	B
5	7.76	H	6.66	V	2.55	H
6	---	---	7.52	T	2.85	T
7	---	---	8.57	V	2.98	B
8	---	---	10.02	B	4.04	H
9	---	---	11.39	B	4.31	T
10	---	---	12.09	B&T	4.51	B
11	---	---	13.89	B&T	---	---

B = longitudinal bending V = transverse bending
T = torsion H = horizontal

Table 2 Natural frequencies of the test bridges.

The fundamental natural frequencies f_1 = 4.44, 3.03 and 1.62 Hz for the Föss, Deibüel and Sort bridge respectively were known from the results of earlier load tests. Their higher natural frequencies and all mode shapes were subsequently precisely determined by

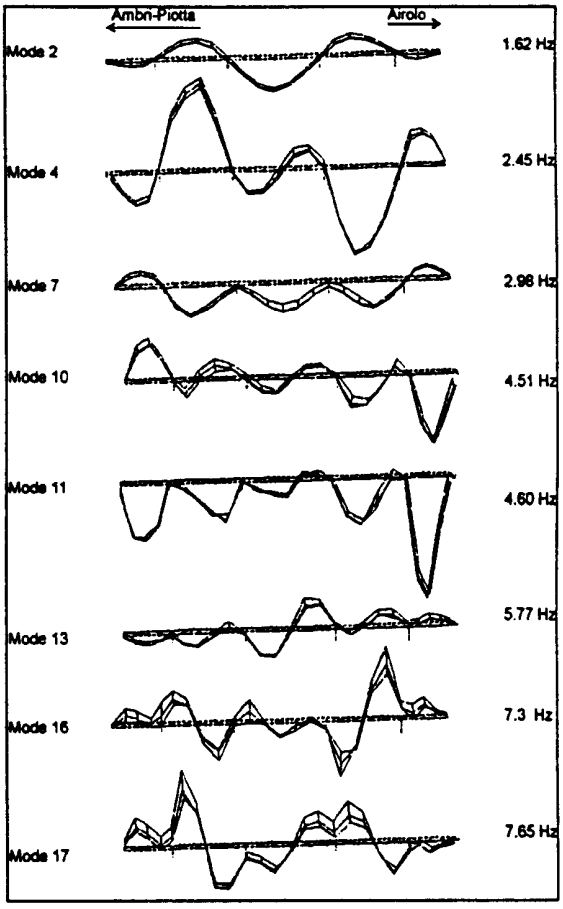

Fig. 3 Some mode shapes of the Sort bridge of the longitudinal bending type.

means of ambient vibration tests performed in 1995 (Table 2, Fig. 3 for the mode shapes of the Sort bridge). With this kind of test, the bridge vibrations excited by the usual traffic are determined and processed in the frequency domain [5], [6].

For the DIVINE tests the bridges were instrumented with inductive displacement transducers to measure vertical deflection. In order to determine the effective vehicle speed, three contact thresholds were fixed to the pavement. One at the start of the test track and the other two at both ends of the bridge.

2.3 The Pavements

The longitudinal pavement profile of the test tracks was measured in both wheel paths by Road Survey Technology Sweden AB (RST), by using the Laser RST Portable Profilometer being mounted on an EMPA car. This measurement system operates with two transducers mounted on a stiff bar fixed to the car's trailer hook. Each consists of a reflective laser sensor contactlessly measuring the distance between the supporting bar and pavement surface plus an accelerometer measuring the acceleration on top of the laser. This acceleration signal is then integrated twice to yield the absolute vertical movement of the laser sensor. The difference in the two signals is the longitudinal pavement profile. The necessary electronics and data acquisition equipment were installed in the car. The measurements were performed at vehicle speeds of v = 35 km/h and v = 70 km/h respectively.

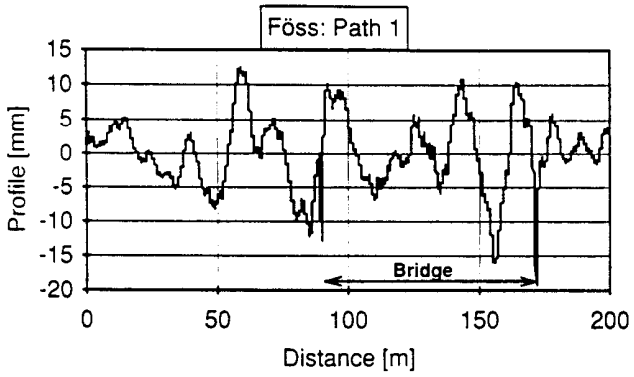

Fig. 4 Pavement profile of the Föss test track. It can be seen that the track consisted not only of the bridge but of a stretch before and after the bridge.

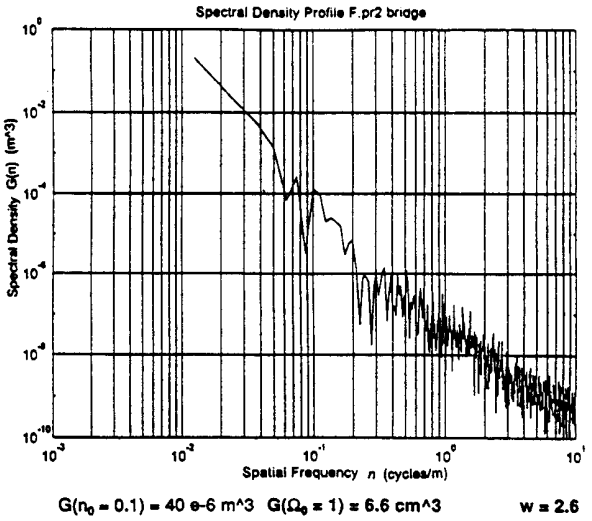

Fig. 5 Unevenness Power Spectral Density of the track given in Figure 4.

Bridge	Path	Gd (Ωo) [x10^{-6} m^3]	Waviness
Deibüel	1	1.8	2.20
	2	2.8	2.10
Föss	1	6.6	2.60
	2	6.6	2.60
Sort	1	1.7	2.00
	2	0.5	2.10

Table 3 Characteristic unevenness Power Spectral Density values of the pavements according to [7].

From the measured profile signals the unevenness power spectra were calculated at the Swedish Road and Traffic Research Institute, VTI, Linköping.

Figures 4 and 5 give an example of the longitudinal profile of the Föss test track and the associated power spectral density diagram as determined by RST and VTI. Table 3 shows the characteristic values of pavement surface unevenness according to ISO [7] for each bridge and wheel path. The pavements were smooth for the Föss, smooth to very smooth for the Deibüel and very smooth for the Sort bridge.

2.4. Test Procedures

The test vehicle was driven over the bridges in their center line. Vehicle speed was kept constant during each specific test and ranged from v = 5 km/h to v = 80 km/h. The usual speed increment from one specific test to the next was Δv = 2 km/h. Tire pressure was kept constant during the tests and was measured at the beginning and at the end of every day. 30 to 50 runs with different speeds were performed at every bridge with both suspension systems. The measurement was started, when the vehicle passed a fixed point, marked by 3 white strips on the pavement, which triggered the data acquisition system. A similar point at the end of the test track stopped the acquisition system. Starting point and end point were placed ≈100 m in front of the beginning of the bridges and ≈100 m after the endpoint of the bridges. The acquired data hence contain 3 sectors: Data taken in front of the bridge, on the bridge and data taken after the bridge.

2.5 Data Acquisition

Two data acquisition systems were operated on-site: a) The NRC MegaDac system plus computer on-board of the test vehicle recorded the wheel-load data and b) the EMPA PCM-system, located in a stationary measurement van, recorded the bridge response. The connection between the two systems was provided by an eight-channel 2.45 GHz radio telemetry link sending the EMPA signals to the NRC MegaDac system. On-line checking of the signals revealed that the telemetry link unfortunately failed after two thirds of the test program had been completed. This lead to some problems when studying the vehicle/bridge interaction behavior. As the exact location of the NRC white strips and of the EMPA contact thresholds are known it should however be possible to cope with these problems.

Two sets of data were hence available after a test: The bridge plus contact threshold signals on the EMPA magnetic tape and all vehicle signals in digitized form on the NRC computer harddisk. When the telemetry link had been working properly, the NRC harddisk data also contained the EMPA signals. The NRC data were copied to an EMPA computer every day.

3. Analysis of the Data

3.1 Analysis in the Time Domain

The dynamic increments as a function of vehicle speed was determined for all bridge measurement instruments and test parameter configurations. The results of these investigations are given in [4].

3.2 Analysis in the Frequency Domain

To determine the wheel load signals and the corresponding power spectra, software packages developed at the National Research Council of Canada (NRC), Ottawa and EDI Ltd., Vancouver were used [8],[9]. With the help of this software it was possible to calculate the power spectra of the wheel loads in an efficient manner. Moreover it is possible to animate the corresponding vibrational mode shapes. With the help of this visual animation it was possible to identify these vibrational shapes.

The analysis was performed in the following steps:

1. Calculating the real wheel loads from the raw data with suitable calibration factors.
2. Splitting the data into separate data sets for every wheel.
3. Defining the lengths of the data for the two parts of the run when I) the vehicle is in front of the bridge and II) the vehicle is on the bridge.
4. Calculating the frequency spectra for the two cases I) and II) for every wheel.
5. Calculating the cross power spectra for the two cases I) and II) for all pairs of wheels.
6. Identifying the peaks and the corresponding frequency in the frequency spectra for every wheel.
7. Plotting the frequencies of the identified peaks in the frequency spectra against velocity for the two cases I) and II) for every wheel.
8. Animating the vibrational shape for all frequencies identified in the frequency spectra and identifying the corresponding mode shape.
9. Plotting the mode shapes and the corresponding frequencies against velocity for the two cases I) and II).

4. Test Results

4.1 Frequency Spectra of Wheel Loads

Figures 6 and 7 show two typical wheel load frequency spectra for steel leaf and air suspension respectively. In these wheel load frequency spectra we find significant peaks at 2.8 Hz in the case of steel leaf suspension and at 1.5 Hz for air suspension. These peaks appear in almost all spectra for every wheel and all velocities. In addition we find peaks at lower frequencies for both suspension systems. The frequency of these peaks often increase with increasing velocity of the vehicle. Additional peaks are seen at higher frequencies up to 10 Hz for steel leaf (Fig. 8) and up to 20 Hz for air suspension (Fig. 9).

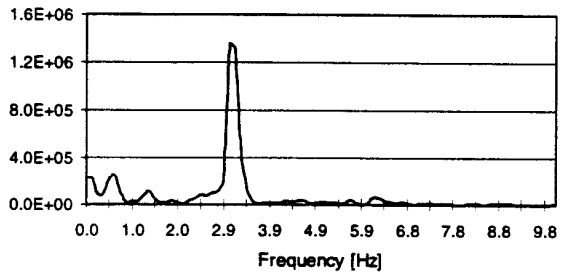

Fig. 6 Example of a wheel load spectral density for steel leaf suspension on Deibüel bridge, wheel No 7, v=37.1 km/h

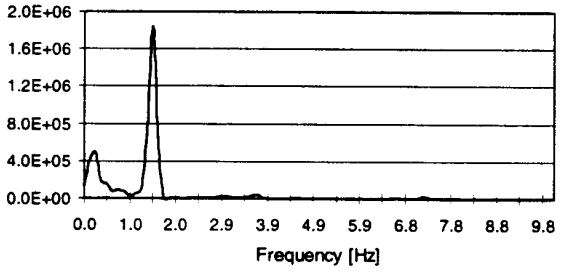

Fig. 7 Example of a wheel load spectral density for air suspension on Deibüel bridge, wheel No 7, v=42.2 km/h

For further analysis we plotted the frequency of the peaks identified in the wheel load spectra against velocity. Figures 10 and 11 show examples for the corresponding scatter plots for steel leaf and air suspension. The lines indicated in the diagrams connect data points corresponding to the most significant peaks in the spectral density plots. In both diagrams we find data depending on velocity and data independent of velocity. The frequency of the velocity dependent part of the data is increasing linearly with velocity. The corresponding scaling factor of the dominant line slope is L = 3.3 m. This line appears in all diagrams for every wheel and both suspension systems. This length corresponds well with the circumference of the wheels of the test vehicle (Table 1). It is hence most probable that this part of the vibration is due to inhomogenities in the wheels of the vehicle.

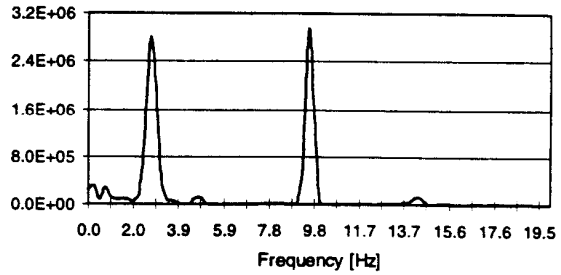

Fig. 8 Example of a wheel load spectral density for steel leaf suspension on Deibüel bridge, wheel No 5, v=57.3 km/h

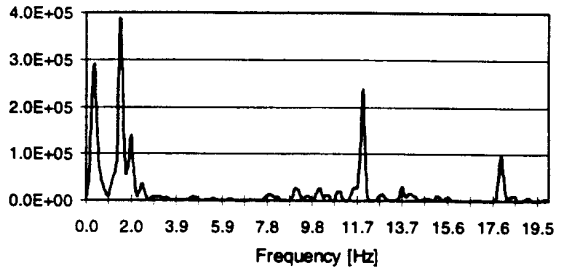

Fig. 9 Example of a wheel load spectral density for air suspension on Sort bridge, wheel No 3, v=70.3 km/h

In addition we find lines with other slopes, corresponding to different lengths. Some of these lengths correspond well to the distances between different pairs of axles of our test vehicle. The distances between different axles of our test vehicle and the characteristic lengths corresponding to the slopes of the observed lines in the wheel load scatter plots are listed in table 4.

Lines with slopes corresponding to distances between axles of the vehicle may be explained due to the so-called 'wheel base filtering': For spatial frequencies of the test track, corresponding to the distance between two axles of the vehicle, the wheels are loaded in phase when the vehicle drives

along the test track. This effect leads to an amplification of the corresponding vibration.

The remaining lines, not corresponding to distances between axles, may be caused due to other peaks in the profiles of the test tracks.

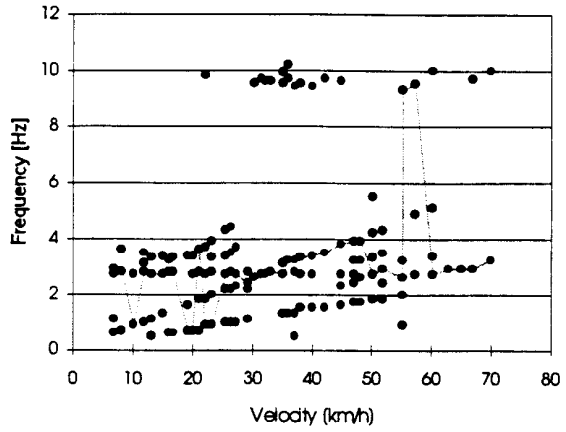

Fig. 10 Frequency of wheel loads vs. velocity for steel leaf suspension on bridge Deibüel, wheel No 5.

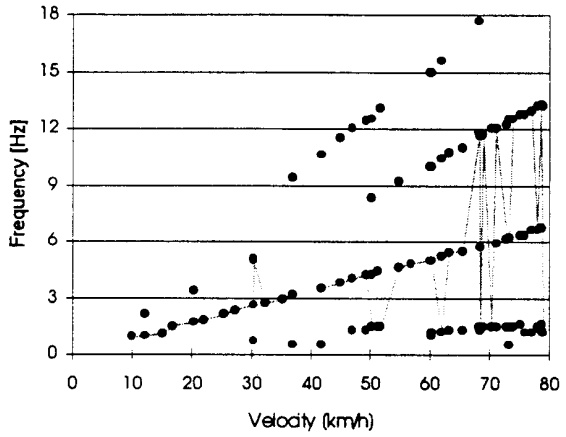

Fig. 11 Frequency of wheel loads vs. velocity for steel leaf suspension on Sort bridge for wheel No 5.

Frequencies that do not depend on velocity are found at 1.5 Hz for air and at 2.8 Hz for steel leaf suspension. In addition, we find peaks which do not depend on the velocity of the vehicle at very low frequencies (< 1.5 Hz) and at high frequencies (10 Hz). In the case of air suspension we find peaks in the wheel load spectra up to 20 Hz that again depend linearly on velocity. No velocity dependent peaks at high frequencies can be seen in the case of steel leaf suspension.

Observed lengths in wheel load diagrams [m]	Distance between axles of the test vehicle [m]	Axles of test vehicle
22.2		
	15.37	1 - 5
14.1	14.00	1 - 4
	12.13	2 - 5
11.1		
10.6	10.76	2 - 4
9.4	9.24	3 - 4
7.8		
5.9		
5.3		
4.8	4.76	1 - 3
3.3	3.28	1 - 2
2.2		
1.6	1.52	2 - 3
1.4	1.37	4 - 5
1.1		
0.9		

Table 4: Observed lengths in wheel load diagrams and distances between axles of the test vehicle.

4.2 Mode Shapes

We identified 12 different types of vibrational modes for the test vehicle. Figure 12 shows the corresponding mode shapes. The 5 axles of the test vehicle are shown schematically and the mode shapes are indicated as relative amplitudes of the ten wheels:

Type 1, 2 and 3 characterize rolling of the vehicle around its longitudinal axis. In type 1 all axles roll in phase. In type 2 there is a phase shift between axles 2/3 and 4/5 of about 90° and in type 3 the phase shift is 180°: the two axle pairs oscillate in opposite direction. Type 4 is the pure heave body bounce vibration, all axles moving up and down in phase. Type 5 is the pure pitch motion of the car body, all axles moving in a plane. Type 6 is a "bending" vibration, the first and the last two axles moving up and down in phase, axles 2 and 3 moving in opposite direction to the first and to the last axles. Type 7 is similar to type 6, but with a phase

shift of about 90° between the twin axles 2/3 and 4/5 respectively. The motion looks similar to the motion of a swimming dolphin.

Types 8, 9 and 10 are axle hop vibrations, with the wheels of the respective axles moving in-phase. Types 11 and 12 are out-of-phase oscillations of the wheels of the twin axles 2/3 and 4/5 respectively with the axis of rotation parallel to the longitudinal axis of the vehicle.

With the help of these 12 types and combinations of them, most vibrational modes could be characterized.

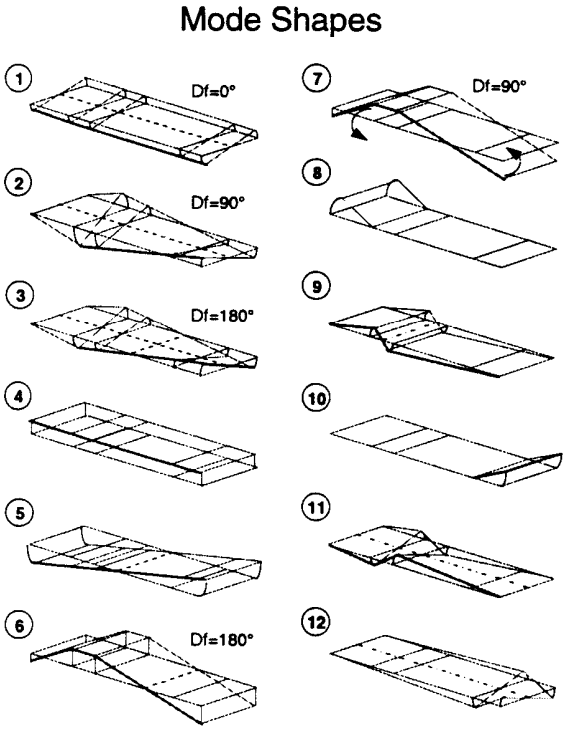

Fig. 12 Mode shapes of the vehicle vibration

Figure 13 and 14 show scatter plots of the mode shapes and the corresponding frequencies versus velocity for steel leaf and air suspension. In both plots we recognize a linear relationship between the frequency and the velocity for part of the data. The slope of the dominant line again corresponds to L = 3.3 m. The vibrational modes change with increasing frequency. At low frequencies the dominant vibrational modes are the rolling types 1, 2 and 3. At medium frequencies (1.5 Hz in the case of air suspension, 2.8 Hz in the case of steel leaf) type 4 is dominant. Type 5, 6 and 7 are found at frequencies in

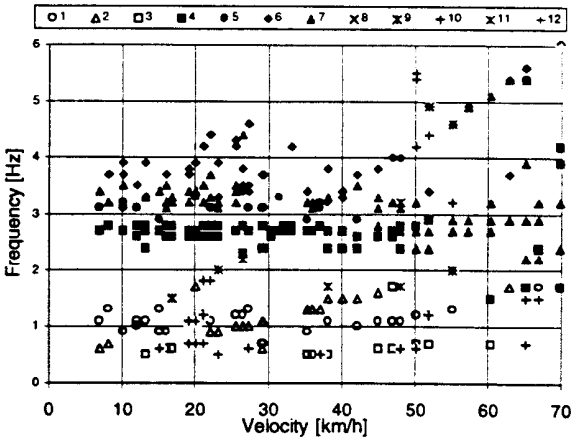

Fig. 13 Frequency of vibrational modes vs. velocity for steel leaf suspension on Deibüel bridge

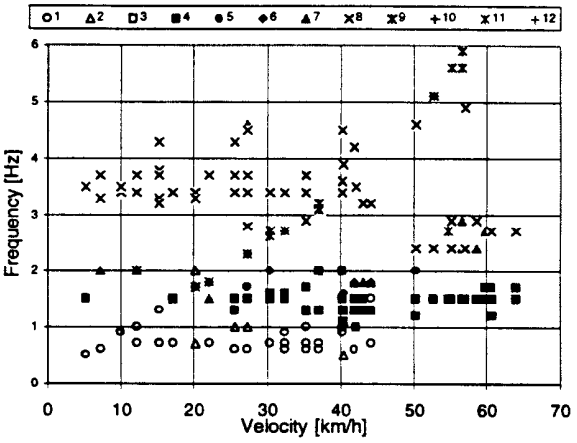

Fig. 14 Frequency of vibrational modes vs. velocity for air suspension on Deibüel bridge

the range f = 3...5 Hz for steel leaf suspension. These mode shapes rarely occur in the case of air suspension. In the same frequency range we find vibration mode 8, only for air suspension. This mode is caused by the fact that the first axle of the vehicle couldn't be changed to air suspension. At 10 Hz we find the mode shapes 9 and 10 (axle hop) independent of velocity for steel leaf suspension and linearly dependent on velocity in the case of air suspension. The slope of the lines corresponds to 1.6 m and 1.1 m. This length is nearly the same as the distance between the axle pairs 2/3 and 4/5 (see table 4). The mode shapes 11 and 12 are exclusively found at highest frequencies (15 to 20 Hz) for air suspension. They couldn't be seen in the case of steel leaf suspension.

4.3 Frequency coupling

When the frequency of the bridge corresponds to the frequency of the vehicle a coupling of the subsystems may occur resulting in a frequency shift of the coupled system. This effect can be observed, when the vehicle with steel leaf suspension (f = 2.8 Hz) passes the Deibüel bridge (f = 3.03 Hz).

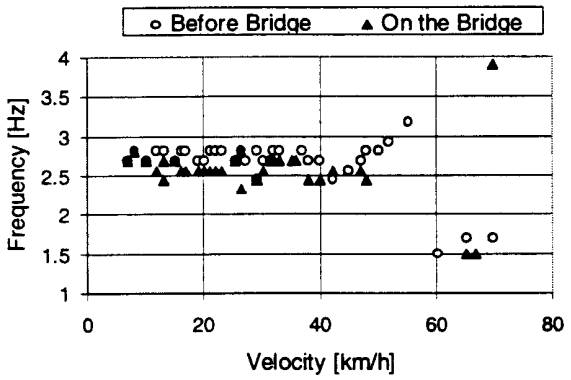

Fig. 15 Frequency vs. velocity of the body bounce vibration (type 4) on the Deibüel bridge for steel leaf suspension.

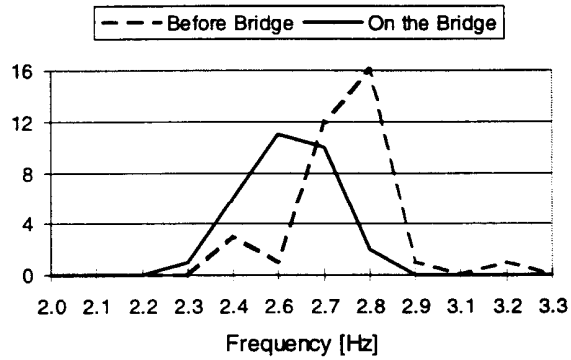

Fig. 16 Histogram of the frequencies of the body bounce vibration on the Deibüel bridge for steel leaf suspension.

Figure 15 shows the frequency versus velocity plot of the pure heave body bounce vibration (type 4) for the vehicle equipped with steel leaf suspension on the bridge Deibüel. Data for the two sectors I) (vehicle is in front of the bridge) and II) (vehicle is on the bridge) are plotted separately. The histogram of the corresponding frequencies is given in Figure 16. The average frequency of vibration is clearly reduced by 0.13 Hz when the vehicle is on the bridge.

Figures 17 and 18 show data for the Deibüel bridge and the vehicle equipped with air suspension. In this case the body bounce frequency of the vehicle is much lower than the lowest frequency of the bridge. No frequency shift can be seen when the vehicle crosses the bridge.

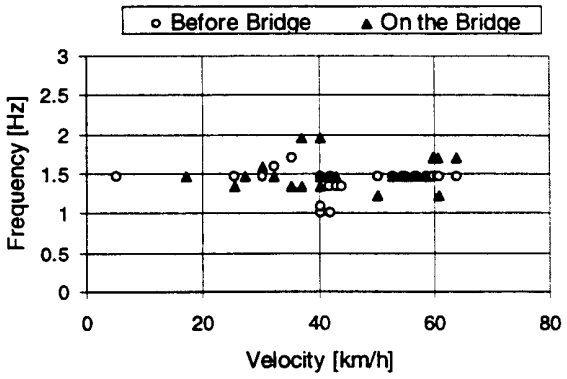

Fig. 17 Frequency vs. velocity of the body bounce vibration (type 4) on the Deibüel bridge for air suspension.

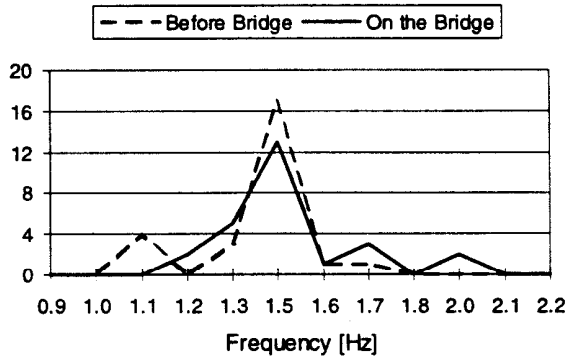

Fig. 18 Histogram of the frequencies of the body bounce vibration on the Deibüel bridge for air suspension.

No effect is seen for the Föss bridge with neither of the two suspension systems. For both suspension systems the frequency of the bridge is much higher than the body bounce frequency of the vehicle. Figures 19 and 20 show the histograms of the corresponding frequencies of the vehicle for the two sectors of the test track - before the bridge and on the bridge - and the two suspension systems.

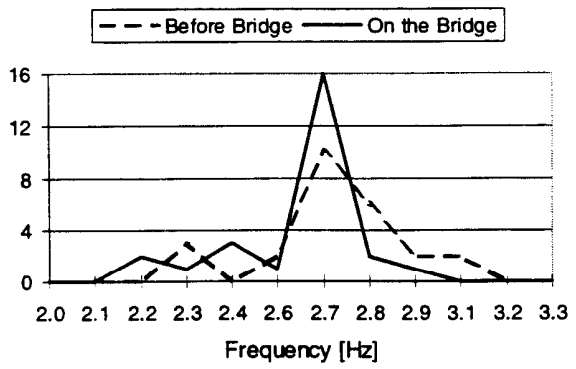

Fig. 19 Histogram of the frequencies of the body bounce vibration on the Föss bridge for steel leaf suspension.

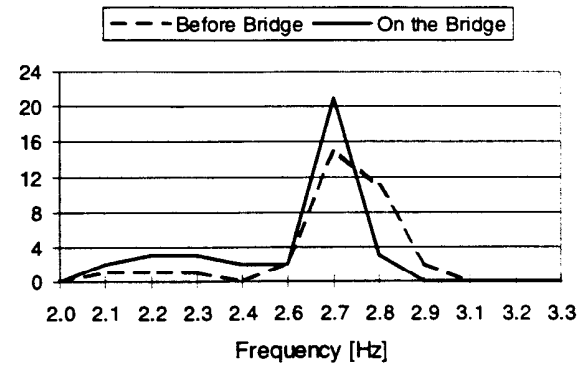

Fig. 21 Histogram of the frequencies of the body bounce vibration on the Sort bridge for steel leaf suspension.

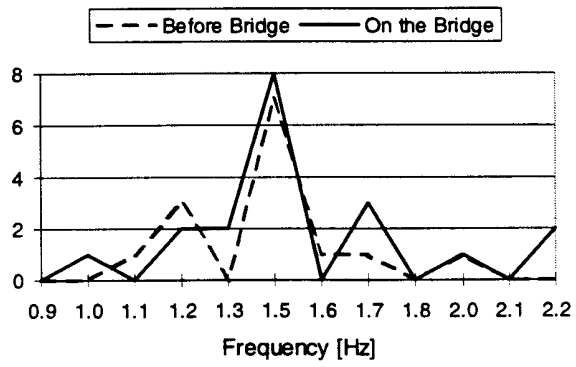

Fig. 20 Histogram of the frequencies of the body bounce vibration on the Föss bridge for air suspension.

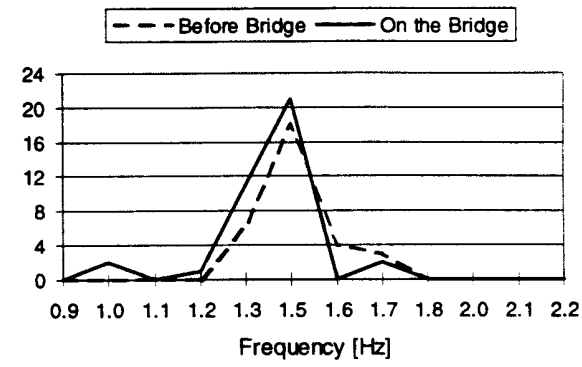

Fig. 22 Histogram of the frequencies of the body bounce vibration on the Sort bridge for air suspension.

At the Sort bridge the situation doesn't show up so clearly. The lowest frequency of the bridge (f_1 = 1.62 Hz) corresponds with the fundamental frequency of the test vehicle equipped with air suspension. But higher bridge mode frequencies (f_2= 2.45 Hz, f_3= 2.98 Hz) are in the range of the fundamental frequency of the vehicle with steel leaf suspension. Our data show a slight frequency shift in the wheel load spectra when the vehicle crosses the bridge compared to the frequency when the vehicle is in front of the bridge for both suspension systems. The frequency resolution Δf= 0.122 Hz, given by the length of the data set in the time domain, the sampling rate and the maximum number of data used by the software, is too poor to separate these peaks. Further investigations will be necessary to confirm that this shift really originates from a frequency coupling of the vehicle with the bridge.

5. Conclusions

As expected, the analysis revealed that frequency coupling of the system vehicle/bridge occurs in the cases, where the fundamental frequencies of the two subsystems are similar, resulting in a reduction in the frequency of the coupled system. This effect is clearly identified, when the test vehicle equipped with steel leaf suspension passes the bridge Deibüel (f_1= 3.03 Hz). The average frequency of the body bounce vibration of the vehicle on the bridge is reduced by Δf= 0.13 Hz compared to the frequency when the vehicle is in front of the bridge and hence frequency coupling occurs during the vehicle's crossing the bridge.

A smaller frequency shift (Δf= 0.05 Hz) is observed, when the vehicle with air spring suspension crosses the Sort bridge, whose fundamental frequency is f_1= 1.6 Hz. Because the mass ratio vehicle/bridge is

much smaller for the larger Sort bridge than for the smaller Deibüel bridge, the expected frequency shift is smaller too.

In addition, a similar effect is observed for the vehicle equipped with steel leaf suspension on the Sort bridge. In this case the natural frequency of the vehicle (f= 2.8 Hz) is higher than the fundamental frequency of the bridge. A possible explanation for this effect could be that frequency coupling with higher natural modes of the bridge might occur. We have, however, to consider that the frequency resolution, limited by the length of the test track on the bridge, is too poor to detect this frequency coupling unambiguously by analyzing the wheel load data of the test vehicle by itself in the case of Sort bridge.

For further investigations data of the bridge response will have to be considered in the analysis too. Knowledge of what bridge modes are actually excited by the vehicle crossing should allow identification of the degree of interaction between vehicle and bridge more clearly.

6. Acknowlegements

The authors wish to thank all persons having been involved in the planning, execution and processing of the tests reported here. Among many others, this includes the colleagues of NRC Canada, VTI Sweden, RST Sweden, TNO Holland, Rijkswaterstaat Holland, TRL United Kingdom, The Technical University of Prague, Czech Republic, AMP Hinwil, EMPA Dübendorf and, last but not least, the members of the OECD IR6 expert group and of the OECD RTR Secretariat, Paris.

We are also indebted to the Highway Administrations of the Cantons Zug and Ticino for helping us to solve the traffic management problems free of any charge.

Thanks to Sara Barella and Andreas Felber, who carried out the first part of data analysis and who supported the authors with their knowledge and experience in vibrational analysis.

For financial support thanks are due to the EMPA Research Council, the EMPA Board of Directors, the National Research Council of Canada and the Swiss Federal Highway Administration representing the Swiss Delegation at OECD RTR.

Special thanks to Prof. Eggiman, President of EMPA, for his interest and his support in this work.

7. References

[1] Cantieni, R., Dynamic Load Tests on Highway Bridges in Switzerland - 60 Years Experience of EMPA. EMPA Report. No. 211 (1983)

[2] Cantieni, R., Dynamic Behavior of Highway Bridges Under the Passage of Heavy Vehicles. EMPA Report No. 220 (1992)

[3] Woodrooffe, J.H.R., LeBlanc, P., LePiane, K.R., Effects of Suspension Variations on the Dynamic Wheel Loads of a Heavy Articulated Highway Vehicle. Vehicle Weights and Dimensions Study (11), Canroad Transportation Research Corporation, Ottawa, Canada (1986)

[4] Cantieni R., Barella S., "Swiss Testing of Medium Span Bridges", Proceedings of the OECD DIVINE Project Mid-Term Seminar, February 2-3, 1995, Sydney, Australia

[5] Felber A.J., "Introduction of a new Ambient Vibration Testing System", EMPA Report No 156'521 (1996)

[6] EMPA Test Report No 153'031/1-2, "Ambient Vibration Study"

[7] Mechanical Vibration - Road Surface Profiles - Reporting of Measured Data. Draft International Standard ISO/DIS 8608, International Organization for Standardization (1991)

[8] Felber, A.J., "Development of a Hybrid Bridge Evaluation System". Ph.D. Thesis, Department of Civil Engineering, University of British Columbia, Vancouver, B.C., Canada (1993)

[9] U2, V2 & P2 Manual Version 2.1. Experimental Dynamic Investigations Ltd. (EDI), Vancouver, B.C., Canada (1995)